Springer

KSME

Journal of Mechanical Science and Technology 32 (12) (2018) 5855~5862
www.springerlink.com/content/1738-494x(Print)/1976-3824(Online)
DOI 10.1007/s12206-018-1134-4

Numerical analysis of distortions by using an incorporated model for welding-heating-cutting processes of a welded lifting lug †

Chao Wang[1] and Jae-Woong Kim[2,*]

[1]*School of Mechanical Engineering, Changshu Institute of Technology, Changshu, 215500, China*
[2]*School of Mechanical Engineering, Yeungnam University, Gyeongsan, Gyeongbuk 38541, Korea*

(Manuscript Received May 30, 2018; Revised September 27, 2018; Accepted October 8, 2018)

Abstract

A lifting lug is a widely used welded structure in the shipbuilding industry. Welded lugs with holes that are attached to heavy blocks are hooked onto and transported by a crane. The lugs are cut away after the heavy blocks are set up at the right position. In this study, a new thermal compensation method was proposed to improve the productivity of removing a lifting lug by band saw cutting. A lifting lug employs a welding process, a heat treatment process, and a cutting process, and thus a coupled 3D finite element model was developed to investigate the distortion and residual stress redistribution during the three processes. The results of the numerical and the experimental studies indicated that the thermal compensation method was effective in improving the productivity of removing the lifting lug. The numerical simulation ensured that the mechanism and influence of various local heating conditions were well illustrated and discussed. It is expected that the coupled finite element model developed in this study can solve practical problems of industrial production.

Keywords: Band saw cutting; Lifting lug; Thermal heating effect; Distortion redistribution; Residual stress redistribution

1. Introduction

Lifting lugs are indispensable welded structures during the transportation of heavy blocks by cranes. After the heavy blocks are set up, it is necessary to remove lifting lugs from the surface. An investigation indicated that it is necessary to operate more than 150000 sets of the lifting lugs by a large shipbuilding factory annually. The 1st cutting, 2nd cutting, milling, grinding, and re-painting processes are incorporated into the cutting process of a lifting lug, and thus only an approximate average of 2 to 3 lifting lugs could be handled by a worker daily. Thus, it is necessary to primarily increase the productivity as well as the sound cutting quality in the cutting process of a lifting lug.

Typically, flame-cutting equipment is used because of its high efficiency and flexibility. The flame cutting procedure includes three stages with respect to the lug cutting process. First, the lifting lug was cut off such that a portion of approximately 25 mm remained, and the surface of block with the heavy block was protected by immersion in water. This was followed by a time consuming milling process to remove the remaining part without the protection by using cutting oil. Finally, the grinding and repainting processes were performed based on the working condition. Excessive heat input induced by flame cutting can certainly enhance the hardness of cutting surface, and this then makes the subsequent milling process considerably more time consuming. Additionally, the painting coat on the heavy block is also harmed by the high temperature as well as unnecessary distortion of the heavy block. Based on the condition, the milling, repainting and thermal straightening processes increase the time consuming process of removing the lifting lug.

Band saw cutting could avoid several problems caused by the flame cutting process, and hence, the band saw cutting was adopted by the shipbuilding factory. However, continuous distortion occurs in the band saw cutting process because of the stress redistribution from the welded residual stresses. The kerf width becomes narrow, and the cutting path curves are accompanied with continuous distortion. Thus, the saw blade is pressed by the material and this induces the stiction problem. The friction shortens the lifetime of the saw blade and sometimes can lead to the failure of the saw blade.

As shown in Fig. 1, a new lug cutting machine was designed by Seon-Kook Jeong based on the viewpoint of alleviating the friction from secondary distortion with an additional function of a self-adapting saw blade. The self-adaption saw blade could change the angle of the blade to fit the curved cutting path. However, it is not possible for this mechanical method to avoid the narrowing of the kerf width, and the stic-

*Corresponding author. Tel.: +82 53 810 2468
E-mail address: jaekim@ynu.ac.kr
† Recommended by Associate Editor Kyeongsik Woo

tion problem continues to occur. Hence, the present study focused on resolving the primary cause of secondary distortion in the cutting process and avoiding the usage of mechanical methods.

The stress state in the machined part is significantly related to the continuous distortion. Wang confirmed that the redistribution of residual stress is the primary reason of machining distortion [1]. Hence, the key to solve the continuous distortion involves conducting stress redistribution in the welded structure. A large tensile stress is produced around the bead, since the lifting lug is welded on the heavy block. The tensile stresses lead to the shrinkage of bead and are partly stored in the weld bead [2, 3]. This stored tensile stress is significantly redistributed during the cutting process and results in a continuous distortion that contributes to secondary distortion. The high temperature on the topside of the lug can induce a large amount of plastic deformation as well as tensile stress. It is expected that the tensile stress in the weld bead will decrease aided by self-equilibrium in the structure. Hence, the primary cause of the continuous distortion could be resolved.

A coupled 3D thermo-elastic-plastic finite element model was developed to study distortion and stress redistribution among the welding process, local heating process, and cutting process. The development of computer technology allows a series of commercial finite element codes to be adopted for the mathematical modeling of the welding/heating process. In the present study, the commercial code MSC. Marc was utilized to conduct all the thermal-mechanical simulations. The 3D elastic-plastic models developed in this study could be used for the simulation of welding, heating, and cutting process. The solution procedure of the thermal-mechanical simulation includes two stages. In the first stage, the temperature distributions at each time step are calculated by the analysis of heat conduction. Deng confirmed that the temperature history obtained at the first stage is then used as the conditions to employ the subsequent mechanical analysis [4]. The function of the pre-state method included transferring data from a previously obtained Marc post file (welding model/ local heating model) to the machining model (band saw cutting model). This pre-state function is extremely useful for saving time and improving the accuracy. In 1945, Merchant first explained the mechanics in a cutting process by considering the plastic behavior of a material [5]. After several years, researchers identified element deformation as the core problem in analyzing the cutting process. Isoparametric 8-node brick elements were used since an option assumed strain interpolation formulation is available for this element. This significantly improves the behavior of this element in bending. The emerging large element distortion is investigated with a Lagrange approach. With applying the function of MSC. Marc, the automatic deactivation method was utilized to simulate the band saw cutting process based on a previous study.

A solution procedure for the stiction problem during removing a lifting had been conducted by numerical simulation of

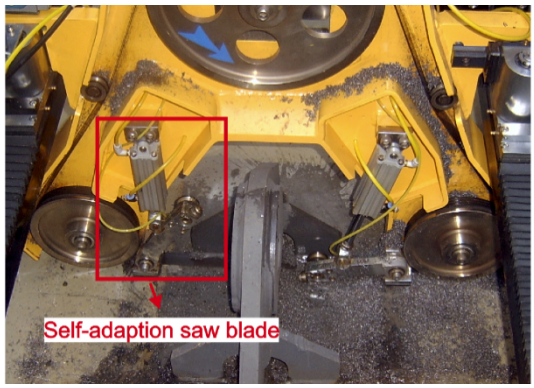

Fig. 1. Band saw machine with self-adaption saw blade.

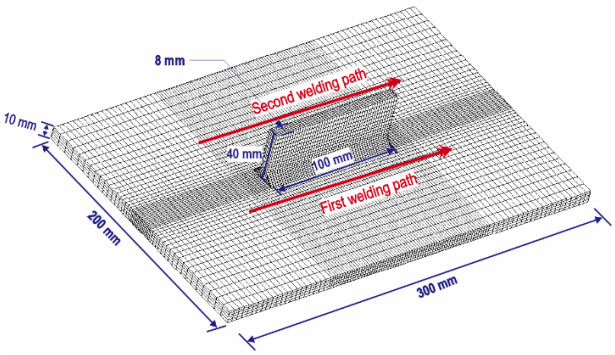

Fig. 2. Mesh of the simplified lug structure with specified size.

stress redistribution. From the previous study by authors, the stored tensile stress around the weld bead was reduced through an additional local heating on the topside of the lug [6]. Thus, the continuous distortion did not occur during the cutting process. Hence, the kerf width did not become narrow, and the cutting path continued straightening. The stiction problem between the saw blade and materials is thereby avoided without employing complicated mechanical methods. A series of experiments based on the simulation was conducted to support the numerical simulation viewpoints sufficiently.

2. Numerical analysis

It is necessary to weld the lifting lug prior to its removal, and a local heating process is considered as added between the welding process and cutting process. A coupled model that could perform the welding simulation, heating simulation, and cutting simulation was developed based on previous studies. Hence, effects of various parameters could be compared in terms of their contribution to optimizing the industrial production. Moreover, the SM400A that is widely used on shipbuilding was defined as the material of the lifting lug. The mesh of the simplified lug structure with a specified size is shown in Fig. 2 with 37180 elements and 44964 nodes. A 3D arbitrarily distorted type 7 element was employed in the study.

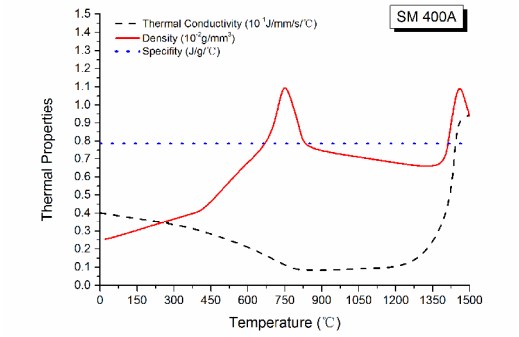

(a)

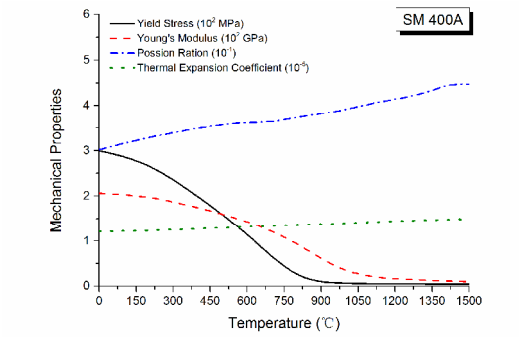

(b)

Fig. 3. Temperature dependent material properties of SM400A: (a) Thermal properties; (b) mechanical properties.

2.1 Features of the coupled finite element model

The 3D solid thermo-elastic-plastic model was employed in the thermal and mechanical analysis of the whole procedure. The element rebirth technology, local adaptive mesh technology, and 321 mechanical constraints were adopted in the coupled model. Temperature-dependent properties are recommended to be used for making an accurate prediction of residual stress distribution [7]. Thus, the temperature dependent material properties were employed and are summarized in Figs. 3(a) and (b). They include the temperature dependent yield stress that was functioned with the von Mises yield criterion.

2.2 Modeling of gas metal arc welding

Successful modeling of the gas metal arc welding process is the primary capability of the coupled finite element model. In order to improve the accuracy of predicting the welding distortion and residual stress distribution of welding process, it is recommended by Perić that the model functioned with element rebirth technology and included a blank gap between the lug and plate would be more accurate [8]. The thickness of the specimens is considerably small, and thus the large deformation theory is employed in the simulation The calculation accuracy and computing time are balanced by designing a fine grid near the weld center and a relatively coarse grid is employed away from the center. The length of the smallest element is approximately 1.25 mm.

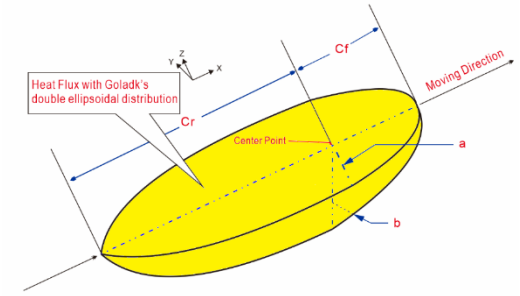

Fig. 4. Model of the Goldak's double ellipsoidal heat source.

The heat transfer analysis was performed by temperature dependent material analysis [9]. The solid-state phase transformation has an insignificant effect in SM400A, and thus it was ignored in the calculation. The spatial and temporal temperature distribution $T(x, y, z, t)$ calculated in the transient heat transfer analysis is given by the governing Eq. (3) as follows:

$$\frac{\partial}{\partial x}\left(k_x\frac{\partial T}{\partial x}\right)+\frac{\partial}{\partial y}\left(k_y\frac{\partial T}{\partial y}\right)+\frac{\partial}{\partial z}\left(k_z\frac{\partial T}{\partial z}\right)+\dot{Q}(x,y,z,t) = \rho c\frac{\partial T}{\partial t}(x,y,z,t) \quad (1)$$

where k_x, k_y and k_z denote the temperature dependent thermal conductivity at x, y and z directions $[\mathrm{J}/(\mathrm{mm}\cdot\mathrm{s}\cdot\mathrm{K})]$, $\dot{Q}$ denotes the heat generation rate $[\mathrm{W}/\mathrm{mm}^3]$, ρ denotes is density $[\mathrm{g}/\mathrm{mm}^3]$, and c denotes the specific heat $[\mathrm{J}/(\mathrm{g}\cdot\mathrm{K})]$.

The material is assumed as isotropic, and thus the temperature dependent thermal conductivity k is the same in the x, y and z directions.

In order to simulate the heat flux from the arc, the Goladk's double ellipsoidal heat source was employed in this welding simulation as plotted in Fig. 4. The heat source model was confirmed to be effective and accurate in the simulation of heat flux by gas tungsten arc(GTA) [10]. The heat flux density decreased from a maximum value in the center, and the total heat input was equivalent to the arc power. The heat source parameters are designed according to the experience and conditioned by the subsequent experiments.

2.3 Modeling of local heating

Arc heating was selected as a local heating method due to its capability of inducting sufficient plasticity deformation on a small plate, and the melting that appears on top side of the lug did not damage the main structure. The heat generation was also simulated by applying Goldak's double ellipsoidal heat source. The simulation of arc heating was performed with three different cases, namely 1.0 kW, 2.5 kW and 3.0 kW. In

Table 1. Experimental sets for the study.

No.	Process procedure
Set 1	Arc welding → Saw cutting
Set 2	Arc welding → Arc heating(1.0 kW) → Saw cutting
Set 3	Arc welding → Arc heating(2.5 kW) → Saw cutting
Set 4	Arc welding → Arc heating(3.0 kW) → Saw cutting

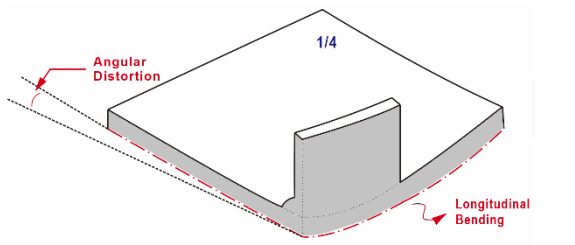

Fig. 5. Position of longitudinal bending and angular distortion.

this stage, the local adaptive mesh technique was used to ensure the accuracy as the topside of the lug had a coarser mesh. Research results of a study by Qingyu et al. suggest that the prediction of temperature fields and displacement distributions are considerably more accurate with the local adaptive mesh technique [11]. Additionally, the calculation time could be significantly reduced by applying this technique.

2.4 Modeling of the band saw cutting process

The pre-state function aids the nodes on the removing surface such that they have initial value of strain ε_i and stress σ_i induced by the previous welding process or local heating process. The automatic deactivation method simulates the disappearance of the elements by forcing the initial strain and stress to zero. This simulation process could also be considered as the release of strains and stresses. Hence, the lug structure experiences a significant change in the stress redistribution and distortion redistribution in the cutting process. The cutting kerf width was selected as 1.8 mm based on the experiment of the band saw cutting process.

3. Experimental procedure

The as-welded case and heated cases with three different power levels were designed to perform the experiments as presented in Table 1. Longitudinal bending deformation and angular distortion were considered as the main welding distortions of the lug structure as identified in Fig. 5. The values were measured by the 3D coordinate measurement machine (CMM) after each process. All the cases were performed by gas metal arc welding. A case involved directly putting them into the band saw cutting process and cutting off the other cases after arc heating on the top side of the lug. The experimental sets are laser cut from as-rolled shipbuilding steel: SM400A.

Table 2. Welding parameters.

Welding current	212 A
Welding voltage	23 V
Welding velocity	308 mm/min
Shielding gas	80 % Ar + 20 % CO_2
Shielding gas flow rate	15 L/min
Electrode wire	HTW – 50, ∅1.2 mm
Travel angle	45°

Fig. 6. Experimental set-up of welding process.

3.1 Process of gas metal arc welding

The gas metal arc welding (GMAW) process yields the coalescence of metals by heating the arc produced between a continuous filler metal electrode and the base metal. The welding set up is shown in Fig. 6. Prior to performing the GMAW, the lug and plate were tack welded by tungsten inert gas arc welding. The duration time between the two weld paths was set as 1800 s. Other welding operating conditions are fixed as shown in Table 2.

Following the welding, the longitudinal bending and angular distortion on the bottom side of the plate were measured by CMM.

3.2 Process of local heating

The arc heating process was performed by a tungsten inert gas welding without filler added. Tungsten inert gas welding uses a non-consumable tungsten electrode to produce the arc for heating. The weld area is protected by inert shielding gas such as argon. As this method was highly developed and could be carried out by automation equipment or manual operation, it is sure to be a quite safe and reliable method.

Experimental set 2 to 4 were arc heated (AH) at the topside of the lug with various arc powers. Additionally, according to the design of the experimental procedure, set 1 was the as-welded (AW) case without the arc heating heat treatment. Sets with arc heating process were measured by CMM again to investigate the distortion redistribution.

3.3 Process of band saw cutting

After that, both the AW set and the AH sets were cut off a 30 mm from the top side of the lug. The set 1 (AW) and sets 2,

Fig. 7. Experimental set-up of band saw cutting process.

3, 4 (AH) were employed with the horizontal band saw machine and the experimental set up was presented in Fig. 7. From the comparison among set 2, 3 and 4, effects from various arc powers during the band sawing process could be investigated. After the band saw cutting process, the redistributed distortion was also measured by CMM and the kerf width variation of each set during band sawing process were recorded each specified cutting length.

4. Results and discussion

4.1 Analysis of welding distortion and residual stress

The welding parameters used in the numerical simulation were consistent with that used in the experiments. The calculated longitudinal bending and angular distortion were compared with the average value from CMM measurements from set 1 to 4. From the Figs. 8(a) and (b), it is observed that the calculated welding distortion showed good agreement with the results of experiments.

The residual stress by the welding process was investigated from the coupled finite element model. Longitudinal residual stress displayed a great relationship with the continuous distortion in the cutting process, since it had a same direction with the welding process, arc-heating process, and cutting process. The magnitude of longitudinal residual stress was distributed from -290 MPa to 390 MPa as presented in Fig. 9(a). Moreover, the stress distribution in the cross section as presented in Fig. 9(b) revealed that the tensile stress was highly concentrated around the weld bead. The equilibrium within the welded structure led to the compressive stresses produced at the topside. With respect to the speculation at the beginning of this study, the tensile stresses contain large elastic shrinkage ability due to the resistance of materials. The calculated stress distribution agreed well with the forementioned point of view.

4.2 Analysis of compensation effect from the local arc heating

Based on the various arc powers, the longitudinal bending deformation of set 2 to 4 were plotted in Figs. 10(a)-(c), respectively. The calculation errors accumulated after two processes, and thus the predicted longitudinal bending after arc

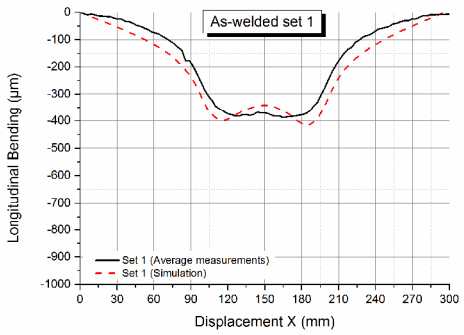

(a)

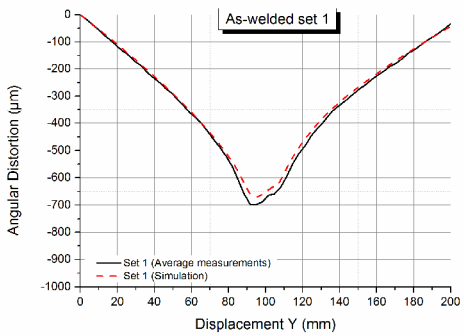

(b)

Fig. 8. A comparison of welding distortion: (a) Longitudinal bending; (b) angular distortion.

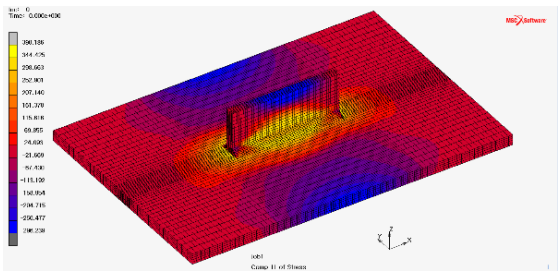

(a)

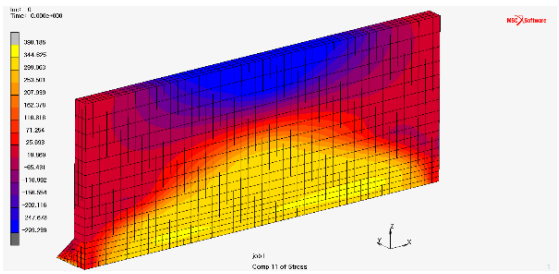

(b)

Fig. 9. Residual stress distribution: (a) Lug structure; (b) cross section of the lug part.

heating was slightly less than that of the corresponding experimental results. The angular distortion was considered to be unchanged by arc heating as indicated by the results plotted in Fig. 11. Additionally, the increase in the longitudinal bending by arc heating displayed a compensation effect on the increas-

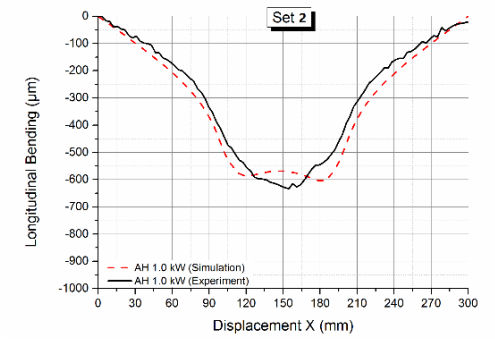

(a)

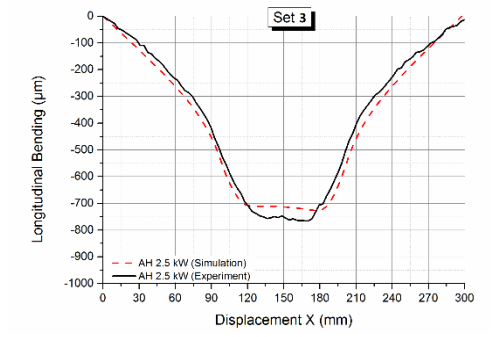

(b)

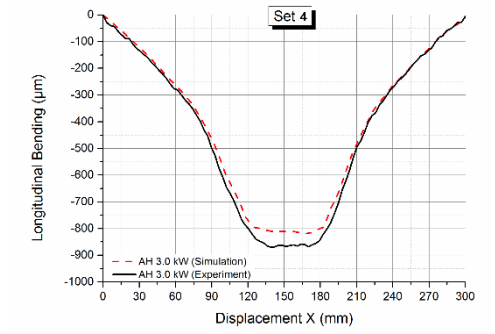

(c)

Fig. 10. Comparison of longitudinal bending after compensation arc heating: (a) Set 2; (b) set 3; (c) set 4.

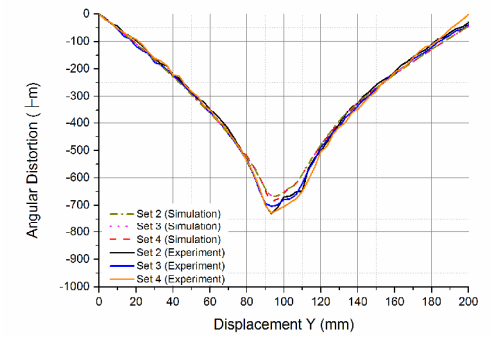

Fig. 11. Comparison of angular distortion after compensation arc heating.

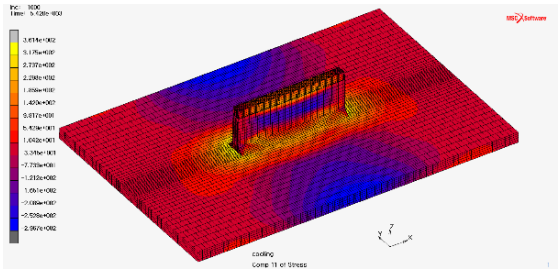

(a)

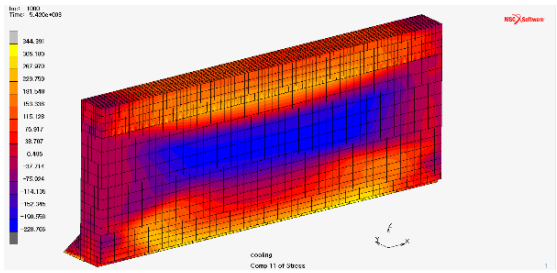

(b)

Fig. 12. Stress distribution after compensation heating: (a) Lug structure; (b) cross section of the lug part.

ing of distortion in cutting the process that increases with the release of shrinkage that is stored in the weld bead.

Ravisankar et al. proposed that longitudinal stress was also significantly redistributed after the arc heating [12]. The longitudinal stresses were redistributed by local arc heating on the topside of the lug as shown in Fig. 12(a). The magnitude of longitudinal stresses within the lug structure did not indicate any significant difference when compared with the residual stress distribution after the welding process. However, the longitudinal stress changed considerably at the top side or around the bead. The compressive stress (-296 MPa max.) at the top side changed into the tensile stress (361 MPa max.) due to the shrinkage induced by arc heating. Additionally, the tensile stress in the weld bead decreased, especially in the center part according to Fig. 12(b). Hence, the stored shrinkage ability around the weld bead that also was the origin of continuous distortion in cutting process decreased with the arc heating. Moreover, the tensile stress that appeared on the topside was supposed to offer a shrinkage force during cutting. Due to the fore-mentioned reasons, the continuous distortion in the cutting process is supposed to decrease and the kerf width is maintained.

4.3 Analysis of the distortions after band saw cutting process

The cutting process was fast and difficult to quantify, and thus the final distortion after cutting process was investigated as opposed to the continuous distortion. Numerical simulation results from AW set 1 and AH sets 2 to 4 are presented in Table 3. The summation continuous distortion in the cutting process was defined as the deformation after cutting that could be simply calculated by the final distortion after cutting process from which the distortion after the previous distortion was

Table 3. Distortion redistribution in the entire experimental procedure.

	Longitudinal bending deformation (μm)			
	After welding	After heating	After cutting	Deformation during cutting
Set 1	415	-	700	285
Set 2		604	690	84
Set 3		727	700	-27
Set 4		765	710	-55

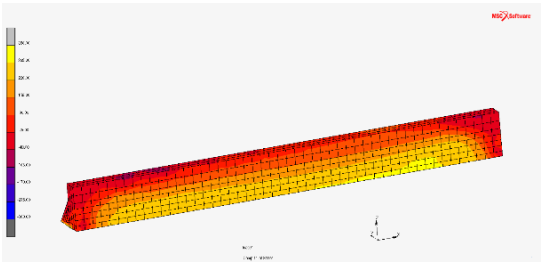

(a)

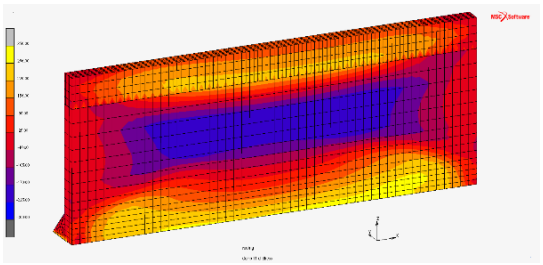

(b)

Fig. 13. Stress redistribution: (a) Without local heating/after cutting; (b) with local heating/before cutting.

deducted. Hence, 285 μm of continuous distortion appears in the cutting process of as-welded process that makes the cutting path curved and induces the stiction problem. However, with the help of 2.5 kW arc heating as set 4, a continuous distortion of only -27 μm appeared. Additionally, the secondary distortion produced by 1.0 kW and 3.0 kW corresponded to 84 μm and -55 μm, respectively. Thus, with an appropriate power, the cutting path continued straightening, and the stiction problem between saw blade and materials could be avoided. This type of a situation was also a good agreement to increase the cutting speed and improve the cutting quality.

The stress distribution around the weld bead is illustrated in Fig. 13. The distribution of the AH set after the arc heating process and the distribution of the AW set after the cutting process are compared, and the results indicated very similar distributions around the weld bead. Thus, the effect of the local arc heating can be understand by both the deformation after cutting viewpoint and the stress redistribution viewpoint.

4.4 Analysis of kerf width variation

The kerf width at the cutting starting position indicates an important role in identifying as to whether or not to squeeze

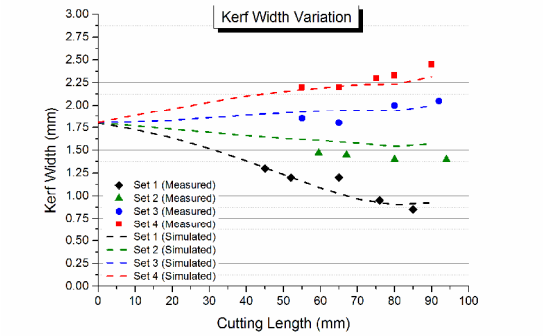

Fig. 14. Kerf width variation in band saw cutting process.

the saw blade. As it is hard to estimate kerf width that related with lots of parameters involved in welding process, local heating process and cutting process. It recommended having a unified coupled model that could predict well through total processes. The calculated results and the experiment-measured results were expressed as a dashed line and points, respectively in Fig. 14.

It was observed that the AW set 1 had an obvious narrowed tendency while the kerf width of AH set 2 to 4 could maintain or even increase in the cutting process. The AW set 1 decreased at approximately 1 mm after cutting a length of 90 mm while the AH set 2 only decreased by 0.4 mm. Additionally, the kerf width of AH set 3 and AH set 4 were increased to 0.3 mm and 0.67 mm, respectively. Arc heating on the topside of the lug decreased the stored shrinkage ability around the weld bead, and a shrinkage force appeared on the topside. Both the factors contributed to maintaining the kerf width in the cutting process as per the results obtained by both the experimental investigations and numerical simulations.

The numerical simulation results predict well with comparing to experiment-measured results. Hence, it was confirmed that the developed unified coupled model could predict welding process, local heating process and cutting process. Which indicate a further appropriate local heating parameter for improving cutting quality during cutting process of a welded structure.

5. Conclusions

The welding process, local heating process, and cutting process could be predicted well by a unified coupled model developed in this study. The numerical simulations on stress distributions after each process allowed an adequate analysis of the mechanism of producing the continuous distortions as well as the prevention method. The main conclusions are as follows:

(1) From the numerical stress analysis, the arc heating on the topside of the lug causes tensile stress at the topside area and decreases the residual tensile stress in weld bead which has the stored shrinkage ability.

(2) Longitudinal bending distortion is increased with the local heating on the topside of lug and the increment is propor-

tional to the heating power.

(3) The stress distribution at the lower part of lug after local heating is very similar to the distribution after cutting with as welded lug. Thus the mechanism of squeezing the band saw at the kerf was identified by these stress analysis.

(4) The incorporated numerical model could also predict the kerf width during band saw cutting process. The prediction ability was verified by comparing the calculation results with the experimental ones.

Thus, it is expected that the incorporated numerical model could be useful for simulating and analyzing multi-step material processing processes and optimizing the precess conditions.

Acknowledgements

This work was supported by the 2018 Yeungnam University Research Grant and Research start-up funds of Changshu Institute of Technology (KYZ2017040Z).

References

[1] Z. Wang, W. Chen, Y. Zhang, Z. Chen and Q. Liu, Study on the machining distortion of thin-walled part caused by redistribution of residual stress, *Chinese J. Aeronaut.*, 18 (2) (2005) 175-179.

[2] D. Venkatkumar and D. Ravindran, 3D finite element simulation of temperature distribution, residual stress and distortion on 304 stainless steel plates using GTA welding, *J. Mech. Sci. Technol.*, 30 (1) (2016) 67-76.

[3] S.-M. Joo, Y.-G. Kim and S.-M. Jeong, Experimental investigation of in-process mitigation of welding distortion for stainless steel plate using air-atomized mist cooling, *J. Mech. Sci. Technol.*, 31 (9) (2017) 4419-4423.

[4] D. Deng, W. Liang and H. Murakawa, Determination of welding deformation in fillet-welded joint by means of numerical simulation and comparison with experimental measurements, *J. Mater. Process. Technol.*, 183 (2-3) (2007) 219-225.

[5] M. E. Merchant, Mechanics of the metal cutting process. II. Plasticity conditions in orthogonal cutting, *J. Appl. Phys.*, 16 (6) (1945) 318-324.

[6] C. Wang and J. W. Kim, A study on the compensation of secondary distortion effect in the cutting process of a welded structure, *J. Mech. Sci. Technol.*, 31 (8) (2017) 3935-3941.

[7] A. R. Kohandehghan and S. Serajzadeh, Arc welding induced residual stress in butt-joints of thin plates under constraints, *J. Manuf. Process.*, 13 (2) (2011) 96-103.

[8] M. Perić, Z. Tonković, I. Garašić and T. Vuherer, An engineering approach for a T-joint fillet welding simulation using simplified material properties, *Ocean Eng.*, 128 (2016) 13-21.

[9] C. Wang, Y. R. Kim and J. W. Kim, Comparison of FE models to predict the welding distortion in T-joint gas metal arc welding process, *Int. J. Precis. Eng. Manuf.*, 15 (8) (2014) 1631-1637.

[10] M. Zubairuddin, S. K. Albert, M. Vasudevan, S. Mahadevan, V. Chaudhari and V. K. Suri, Numerical simulation of multi-pass GTA welding of grade 91 steel, *J. Manuf. Process.*, 27 (2017) 87-97.

[11] S. Qingyu, L. Anli, Z. Haiyan and W. Aiping, Development and application of the adaptive mesh technique in the three-dimensional numerical simulation of the welding process, *J. Mater. Process. Technol.*, 121 (2-3) (2002) 167-172.

[12] A. Ravisankar, S. K. Velaga, G. Rajput and S. Venugopal, Influence of welding speed and power on residual stress during gas tungsten arc welding (GTAW) of thin sections with constant heat input: A study using numerical simulation and experimental validation, *J. Manuf. Process.*, 16 (2) (2014) 200-211.

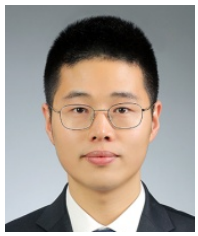

Chao Wang was born in Jiangyin, China. He received his Ph.D. degree at the Graduate School of Yeungnam University, Korea. Now, he is currently working at Changshu Institute of Technology. His areas of research interest include finite element analyses of welding and heat treatment of steel structures.

Jae-Woong Kim received his B.Sc. degree from Ajou University, Korea, in 1982. He received his M.Sc. and Ph.D. degrees in Mech. and Production Eng. from Korea Advanced Institute of Science and Technology, in 1984 and 1991, respectively. He is currently a Professor at the School of Mechanical Eng., Yeungnam University, Korea. His research interests include analysis of welded structures, thermal stress and distortion.